

Factors that influence the antiproliferative activity of half sandwich Ru^{II}-[9]aneS₃ coordination compounds: activation kinetics and interaction with guanine derivatives.

Ana Rilak,^{1,2} Ioannis Bratsos,^{*2} Ennio Zangrando,² Jakob Kljun,³ Iztok Turel,³ Živadin D. Bugarčić,¹
Enzo Alessio,^{*2}

¹ Faculty of Science, University of Kragujevac, R. Domanovića 12, P. O. Box 60, 34000 Kragujevac, Serbia.

² Dipartimento di Scienze Chimiche e Farmaceutiche, Università di Trieste, Via L. Giorgieri 1, 34127 Trieste, Italy.

³ Faculty of Chemistry and Chemical Technology, University of Ljubljana, Aškerčeva c. 5, SI-1000 Ljubljana, Slovenia.

Supplementary Information

[Ru([9]aneS₃)(bpy)Cl](PF₆) (2). To a 100 mg amount of [Ru([9]aneS₃)(dmso-S)₂Cl](PF₆)¹ (0.16 mmol) partially dissolved in 10 mL of methanol 2,2'-bipyridine (25.6 mg, 0.16 mmol) was added and the mixture was refluxed for 1 h. During this time the colour of the solution changed from yellow to orange and the formation of the product as deep yellow solid was observed. After cooling down at ambient temperature, the solid was collected by filtration, washed with ethanol and diethyl ether and vacuum dried (69.4 mg, 70%). Found: C, 30.98; H, 3.07; N, 4.38%. C₁₆H₂₀ClF₆N₂PRuS₃ (618.03) requires: C, 31.09; H, 3.26; N, 4.53%. The spectral patterns of this compound are coincident with those of the corresponding CF₃SO₃ salt.² δ_H (500 MHz; CD₃NO₂) 9.08 (2 H, d, *J* 5.4 Hz, C⁶H/C^{6'}H), 8.48 (2 H, d, *J* 8.1 Hz, C³H/C^{3'}H), 8.14 (2 H, t, *J* 7.9 Hz, C⁴H/C^{4'}H), 7.63 (2 H, t, *J* 6.9 Hz, C⁵H/C^{5'}H), 3.13 – 2.50 (12 H, m, CH₂ [9]aneS₃). δ_H (500 MHz; D₂O) 9.05 (2 H, d, *J* 5.6 Hz, C⁶H/C^{6'}H), 8.47 (2 H, d, *J* 8.3 Hz, C³H/C^{3'}H), 8.13 (2 H, t, *J* 7.7 Hz, C⁴H/C^{4'}H), 7.63 (2 H, t, *J* 6.5 Hz, C⁵H/C^{5'}H), 3.08 – 2.47 (12 H, m, CH₂ [9]aneS₃).

¹ I. Bratsos, E. Mitri, F. Ravalico, E. Zangrandino, T. Gianferrara, A. Bergamo and E. Alessio, *Dalton Trans.*, 2012, **41**, 7358–7371.

² B. Serli, E. Zangrandino, T. Gianferrara, C. Scolaro, P. J. Dyson, A. Bergamo and E. Alessio, *Eur. J. Inorg. Chem.*, 2005, 3423–3434.

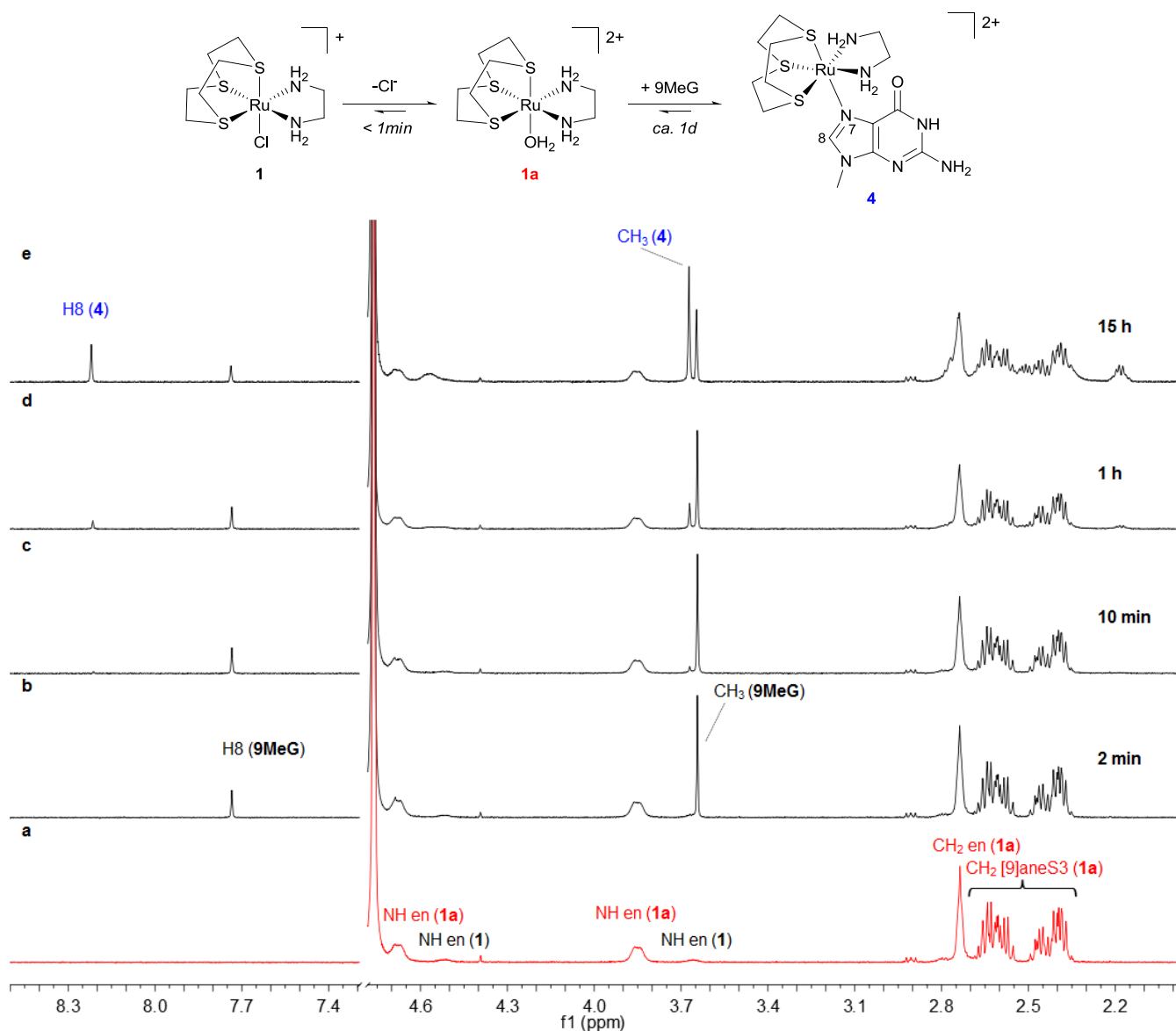


Figure S1. ¹H NMR spectra of [Ru([9]aneS₃)(en)Cl]⁺ (**1**) (4 mM, pH 7.60, 298 K) 5 min after dissolution in D₂O (a) and at various time intervals (b-e) after addition of 9MeG (1:1).

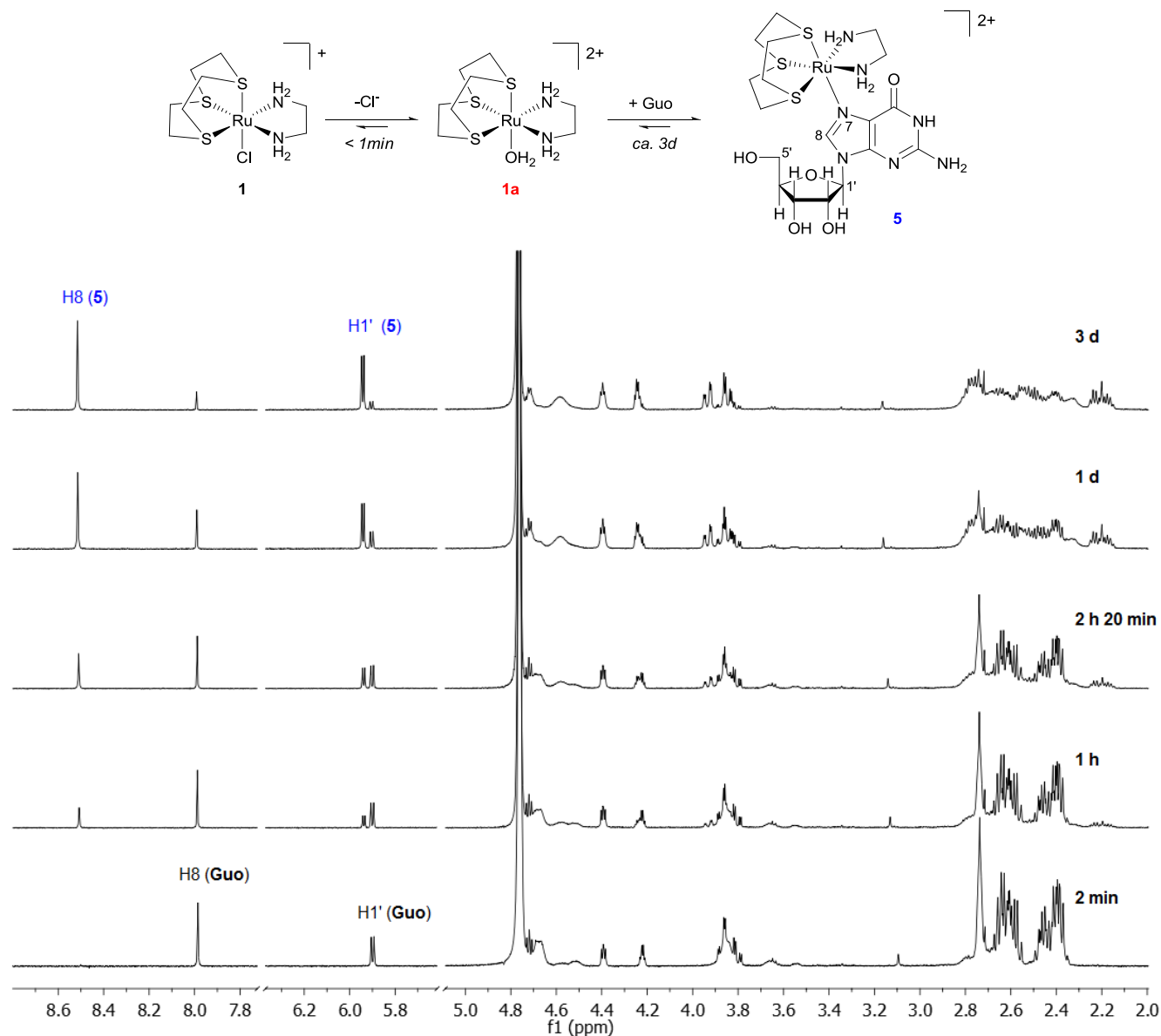


Figure S2. Time evolution of the ¹H NMR spectra of the reaction between Guo and $[\text{Ru}([9]\text{aneS}_3)(\text{en})\text{Cl}]^+$ (**1**) (1:1, 4 mM, D₂O, pH 7.63, 298 K).

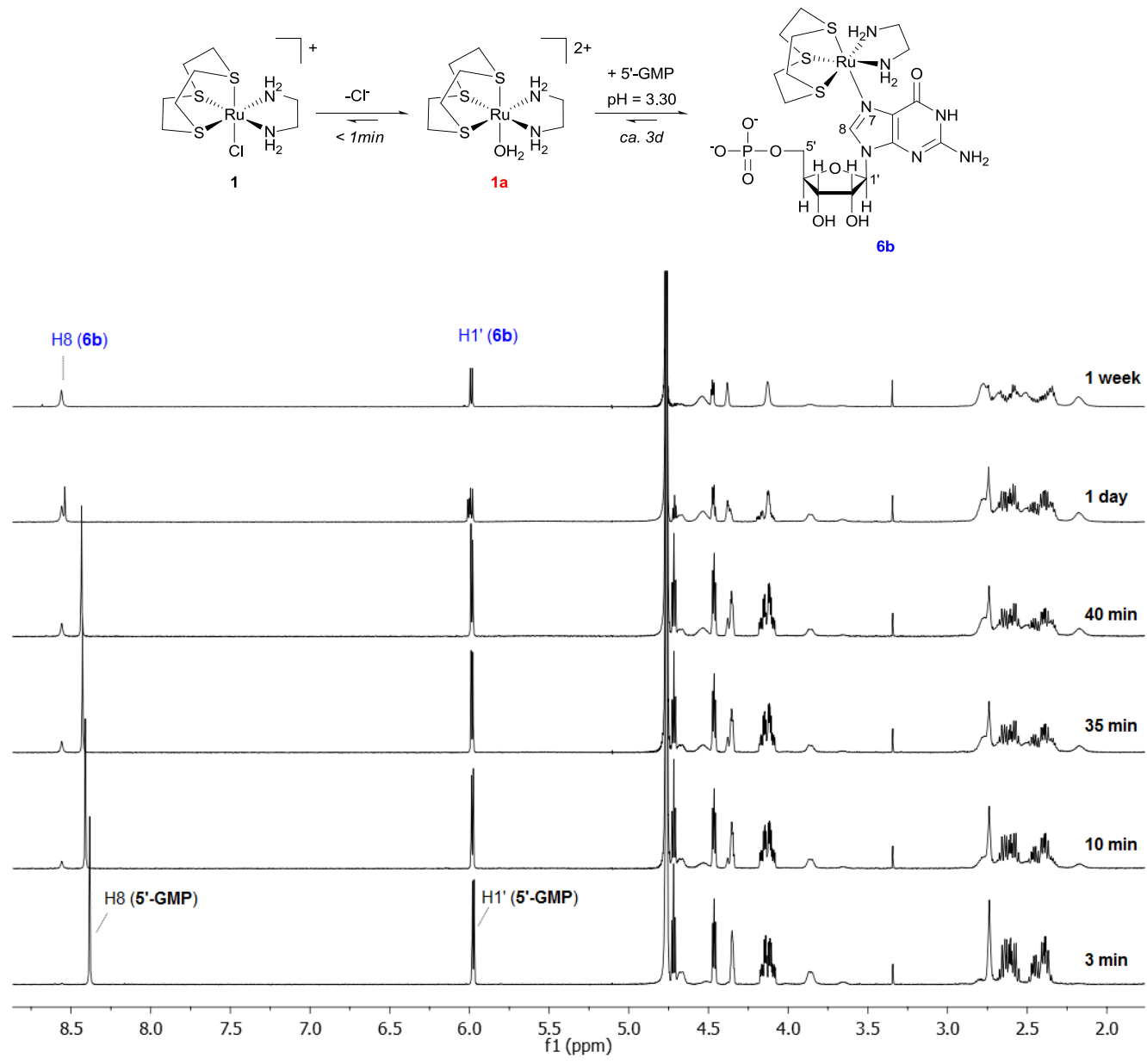


Figure S3. ¹H NMR spectra for the reaction between [Ru([9]aneS₃)(en)Cl]⁺ (**1**) and 5'-GMP (1:1, 10 mM, D₂O, pH 3.30, 298 K) at various reaction times.

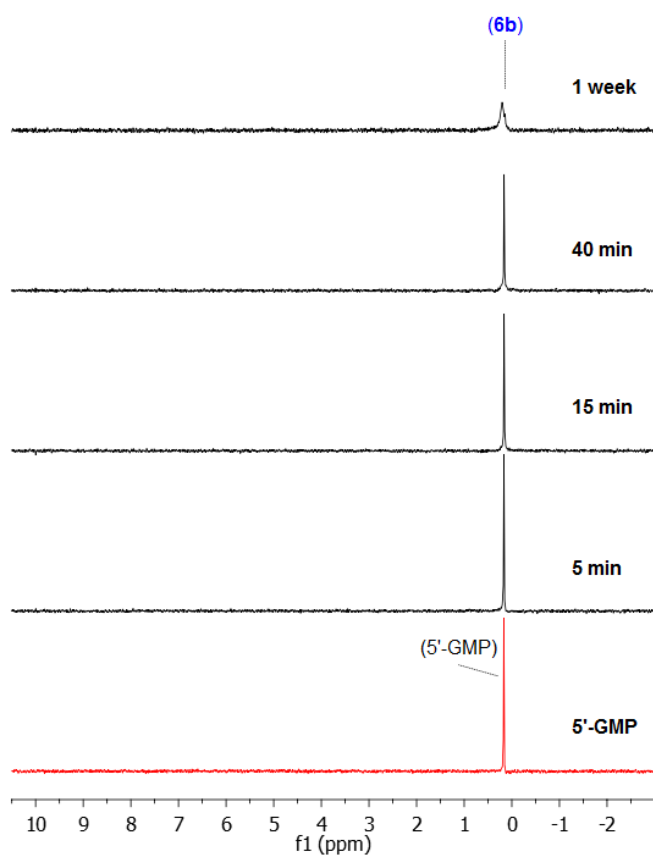


Figure S4. ^{31}P NMR spectra for the reaction between $[\text{Ru}(\text{[9]aneS}_3)(\text{en})\text{Cl}]^+$ (**1**) and 5'-GMP (1:1, 10 mM, D_2O , pH 3.30, 298 K) at various reaction times.

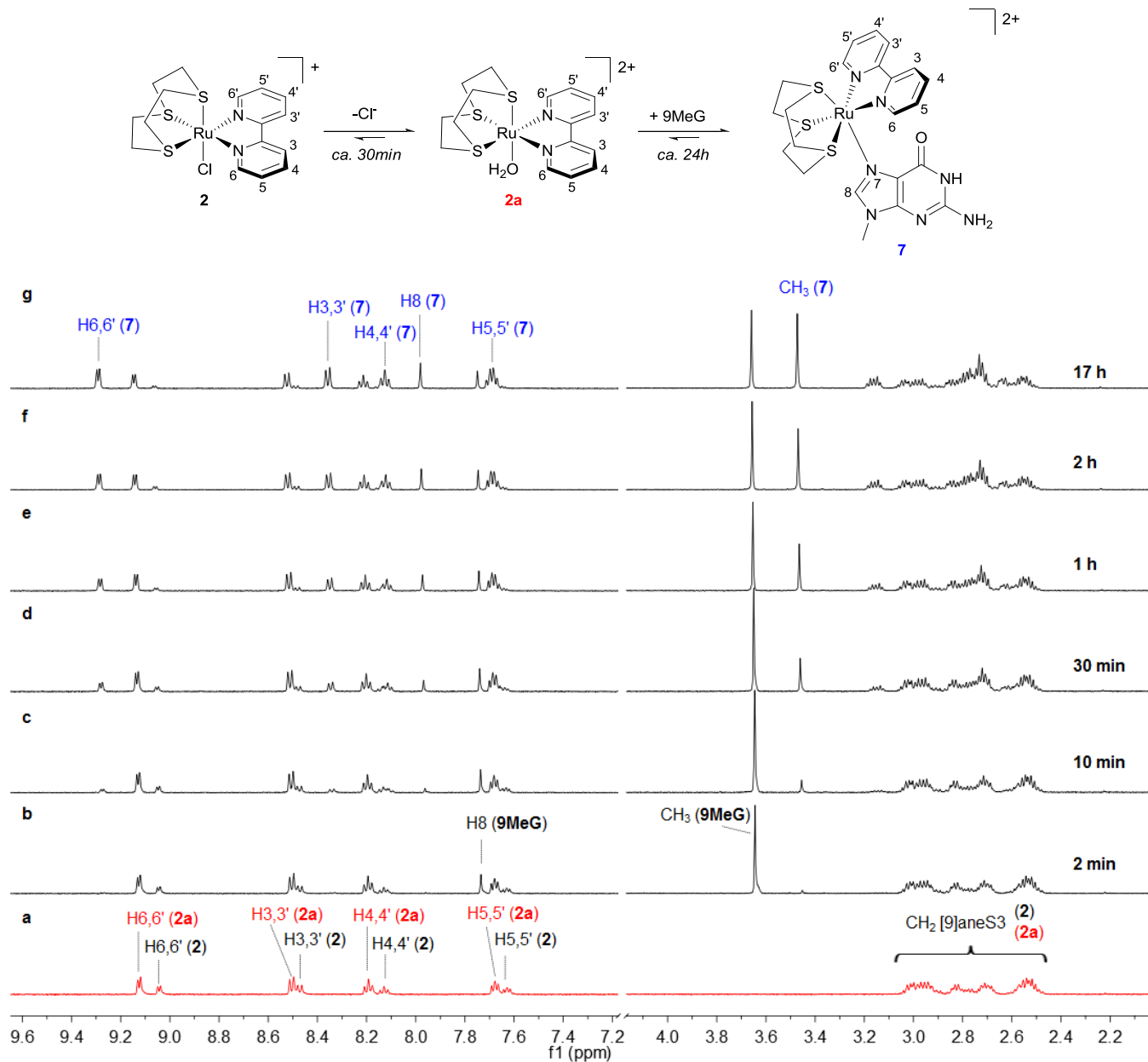


Figure S5. ^1H NMR spectra of $[\text{Ru}(\text{[9]aneS}_3)(\text{bpy})\text{Cl}]^+$ (**2**, 4 mM) in D_2O 30 min after dissolution (a), and after addition of 9MeG (1:1, pH 7.88, 298 K) at various time intervals (b-g).

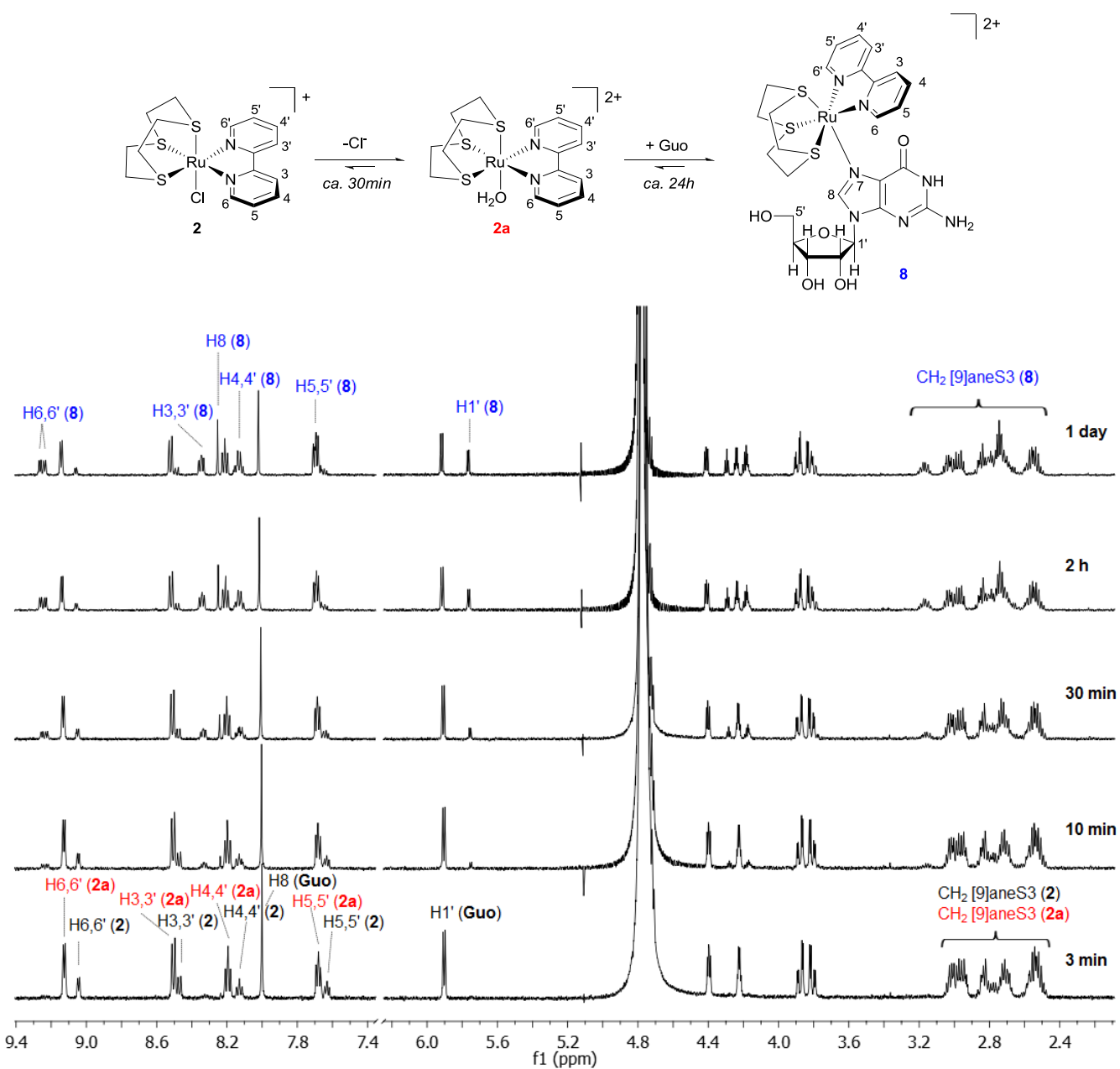


Figure S6. ¹H NMR spectra for the reaction between [Ru([9]aneS₃)(bpy)Cl]⁺ (**2**, 4 mM, 30 min after dissolution) and Guo (1:1, pH 7.74, 298 K) at various reaction times.

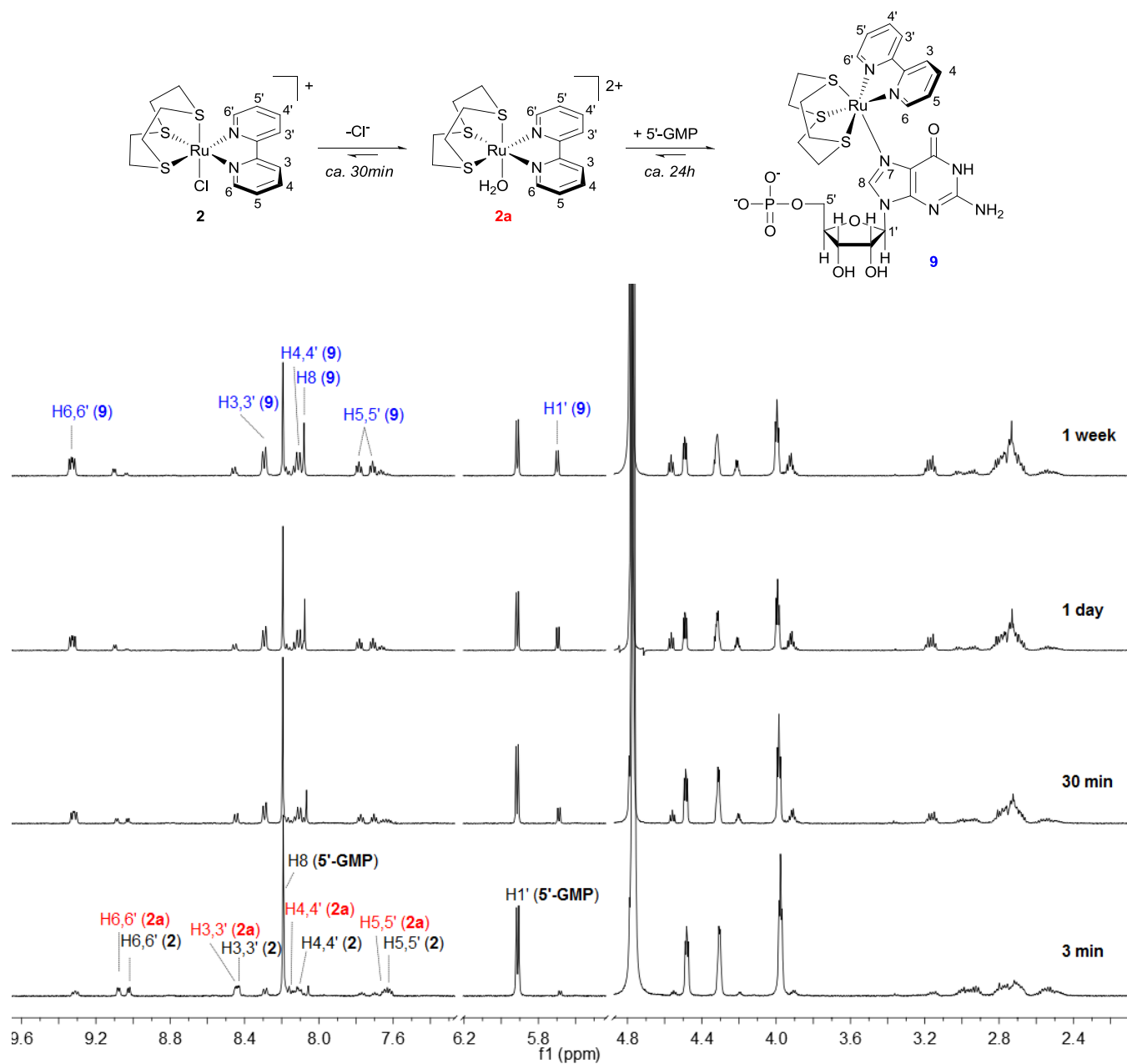


Figure S7. ¹H NMR spectra for the reaction between $[\text{Ru}([\text{9}]\text{aneS}_3)(\text{bpy})\text{Cl}]^+$ (**2**, 10 min after dissolution) and 5'-GMP (1:1, 10 mM, D₂O, pH 7.65, 298 K) at various reaction times.

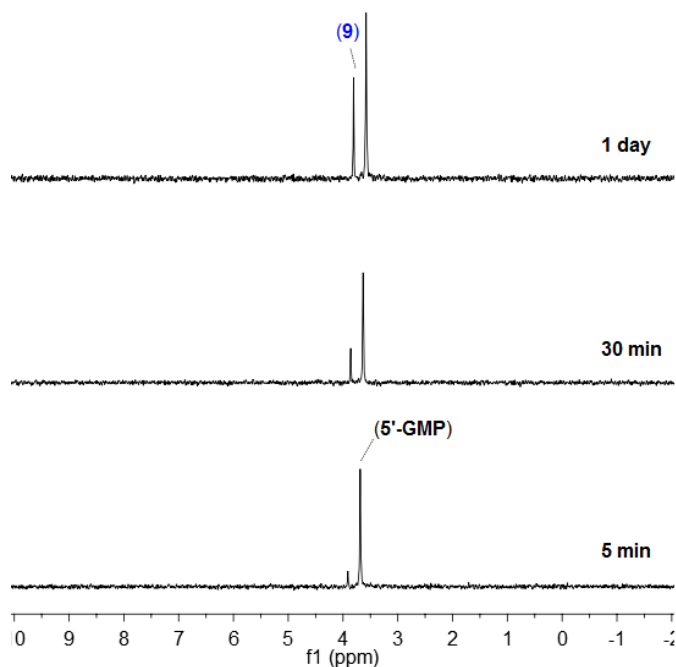


Figure S8. ^{31}P NMR spectra for the reaction between $[\text{Ru}(\text{[9]aneS3})(\text{bpy})\text{Cl}]^+$ (**2**) and 5'-GMP (1:1, 10 mM, D_2O , pH 7.65, 298 K) at various reaction times.

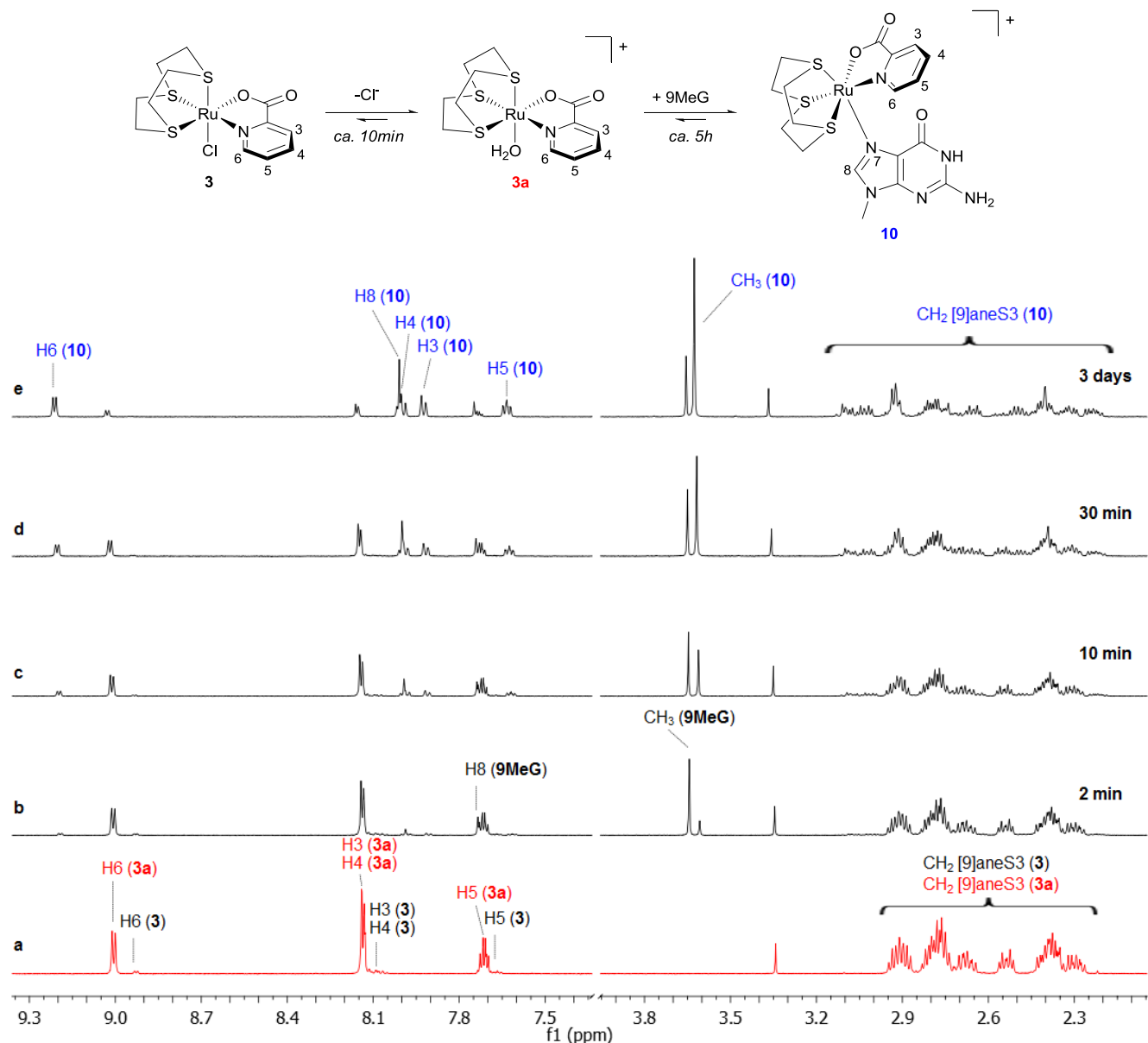


Figure S9. ¹H NMR spectra of [Ru([9]aneS₃)(pic)Cl] (**3**, 4 mM) in D₂O 10 min after dissolution (a), and after addition of 9MeG (1:1, pH 7.73, 298 K) at various time intervals (b-e).

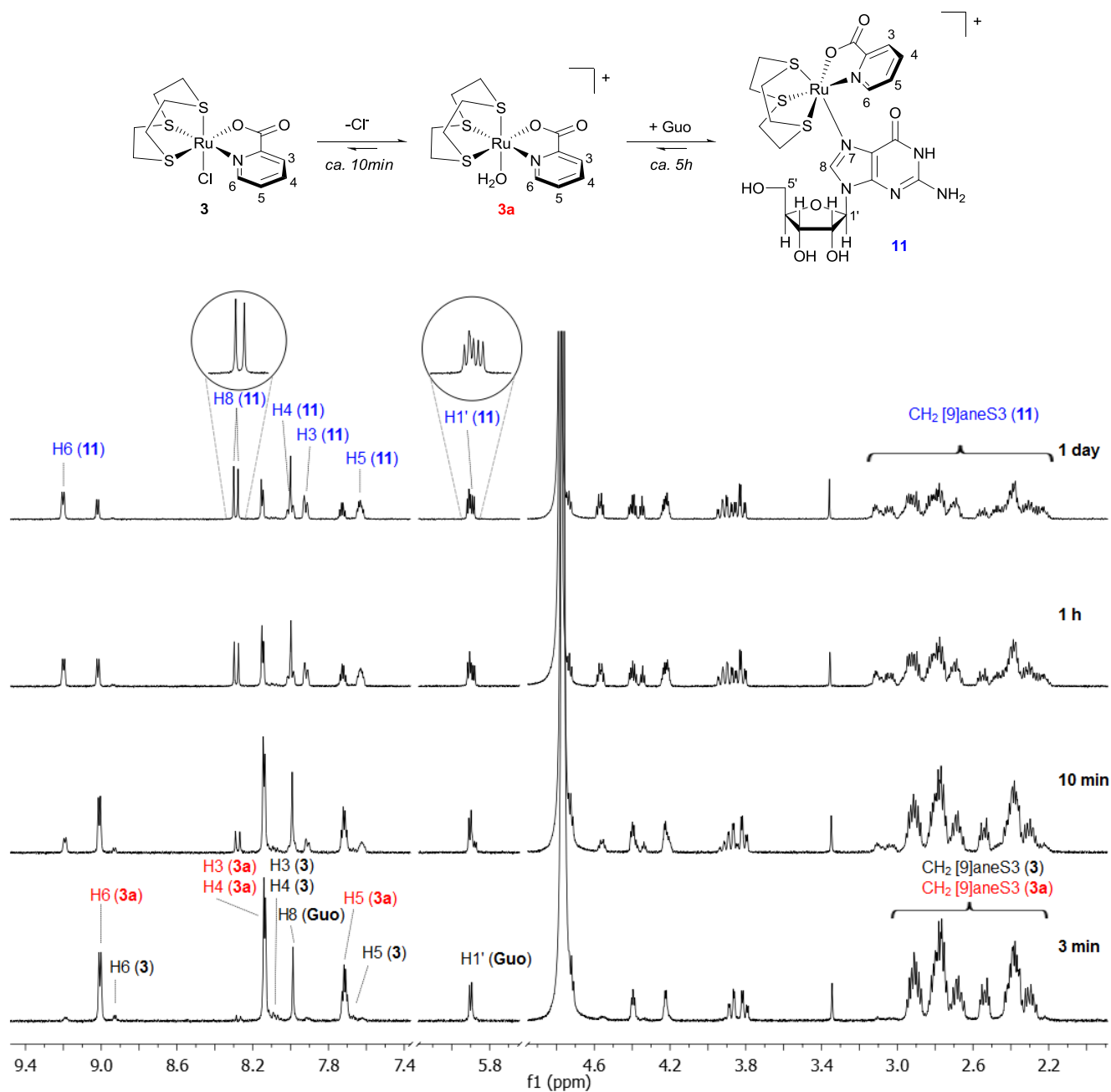


Figure S10. ¹H NMR spectra for the reaction between $[\text{Ru}([\text{9}] \text{aneS3})(\text{pic})\text{Cl}]^+$ (**3**, 10 min after dissolution) and Guo (1:1, 4 mM, D₂O, pH 7.70, 298 K) at various reaction times. The circular insets contain the H8 and H1' resonances of **11** magnified.

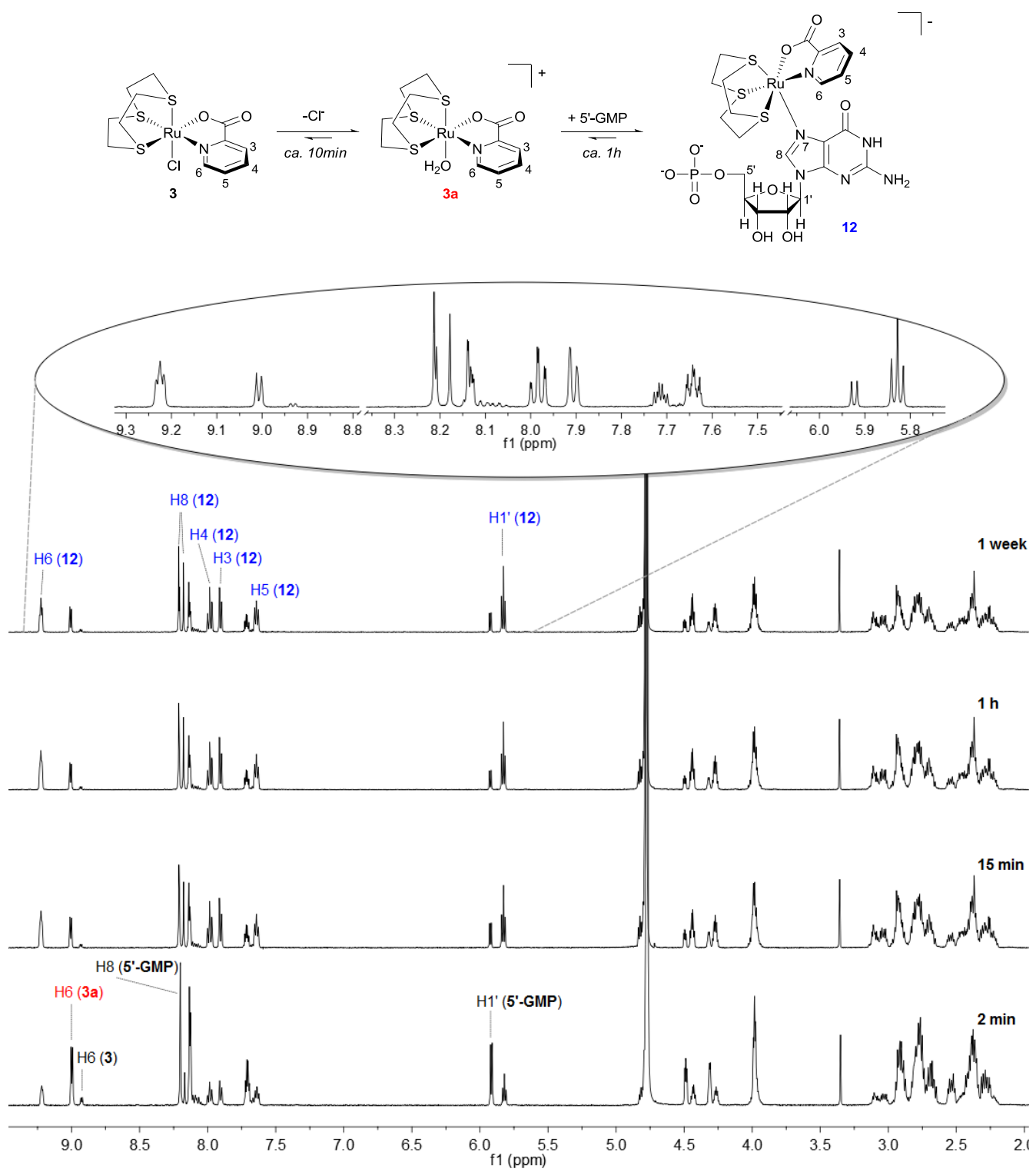


Figure S11. ^1H NMR spectra for the reaction between $[\text{Ru}(\text{9-anS3})(\text{pic})\text{Cl}]^+$ (**3**, 10 min after dissolution) and 5'-GMP (1:1, 10 mM, D_2O , pH 7.95, 298 K) at various reaction times. The oval inset shows the magnified downfield region of the spectrum after 1 week.

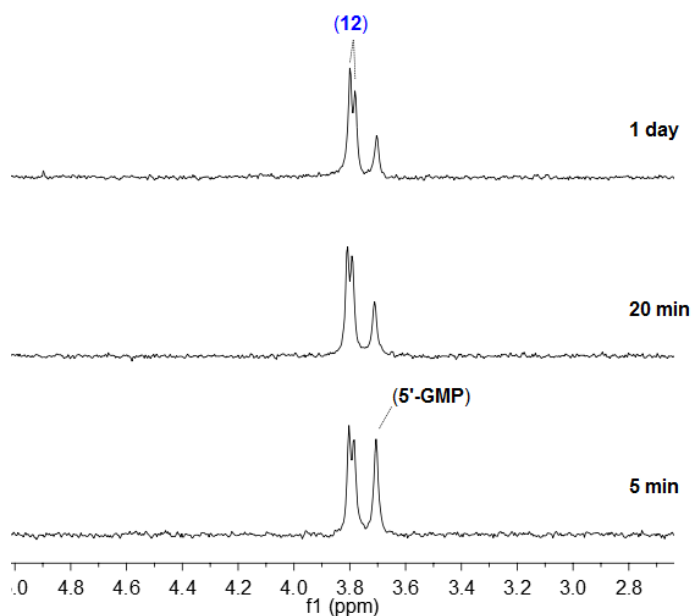


Figure S12. ^{31}P NMR spectra for the reaction between $[\text{Ru}(\text{9-janeS3})(\text{pic})\text{Cl}]^+$ (**3**) and 5'-GMP (1:1, 10 mM, D_2O , pH 7.95, 298 K) at various reaction times.

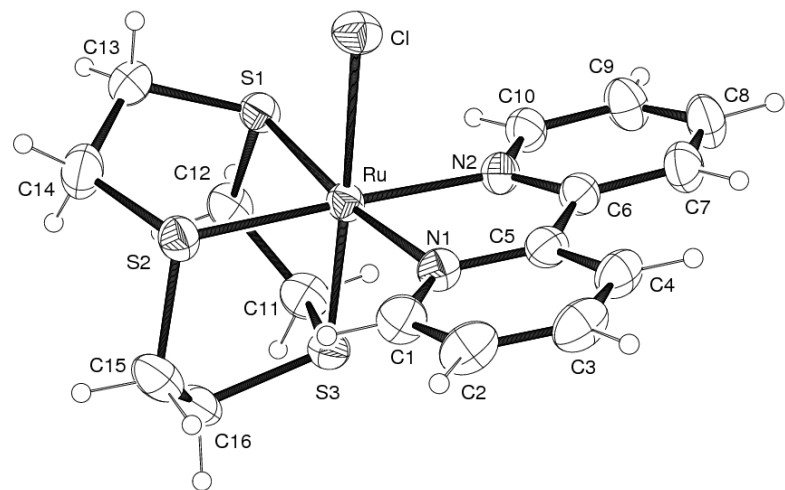


Figure S13. ORTEP view (30% probability ellipsoids) of the cation of $[\text{Ru}([\text{9}] \text{aneS}_3)(\text{bpy})\text{Cl}](\text{PF}_6)$ (**2**) with atom labelling scheme. Selected bond lengths (\AA) and angles ($^\circ$): Ru–N(1) 2.103(3), Ru–N(2) 2.093(3), Ru–S(1) 2.2965(9), Ru–S(2) 2.3027(9), Ru–S(3) 2.2830(9), Ru–Cl 2.4338(9); N(1)–Ru–N(2) 77.68(11), N(1)–Ru–Cl 86.51(8), N(1)–Ru–S(1) 172.67(8), N(1)–Ru–S(2) 97.11(8), N(1)–Ru–S(3) 97.87(8), N(2)–Ru–Cl 87.17(8), N(2)–Ru–S(1) 97.77(8), N(2)–Ru–S(2) 174.65(8), N(2)–Ru–S(3) 93.35(8), S(1)–Ru–S(2) 87.29(3), S(1)–Ru–S(3) 88.07(3), S(2)–Ru–S(3) 88.52(4), S(1)–Ru–Cl 87.54(3), S(2)–Ru–Cl 91.34(4), S(3)–Ru–Cl 175.61(3).

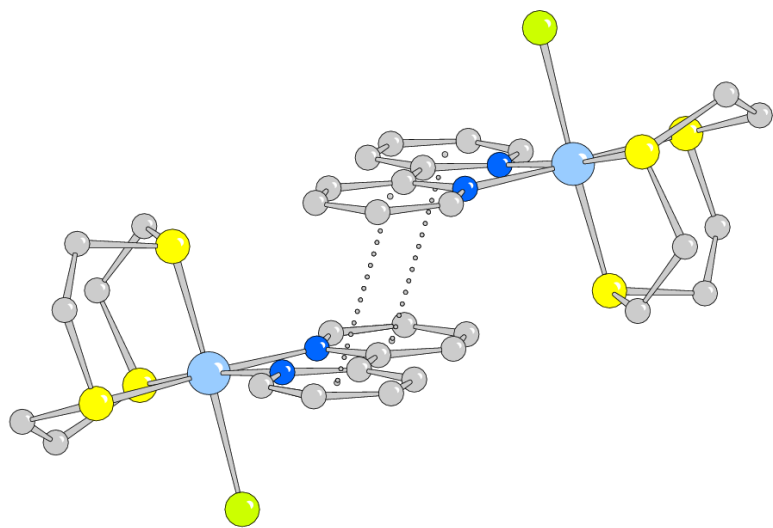


Figure S14. The centrosymmetric arrangement in the crystal of complex **2**.

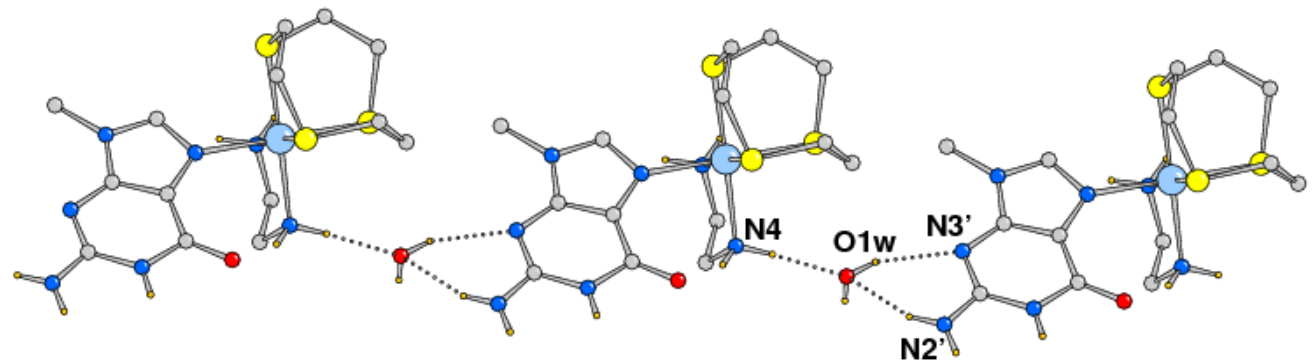


Figure S15. Crystal packing of complex $[\text{Ru}([\text{9}] \text{aneS3})(\text{en})(\text{9MeG-}N7)](\text{PF}_6)_2$ (**4**): the lattice water molecule connects metal complexes through H-bonds giving rise to a 1D chain along the *b*-axis.

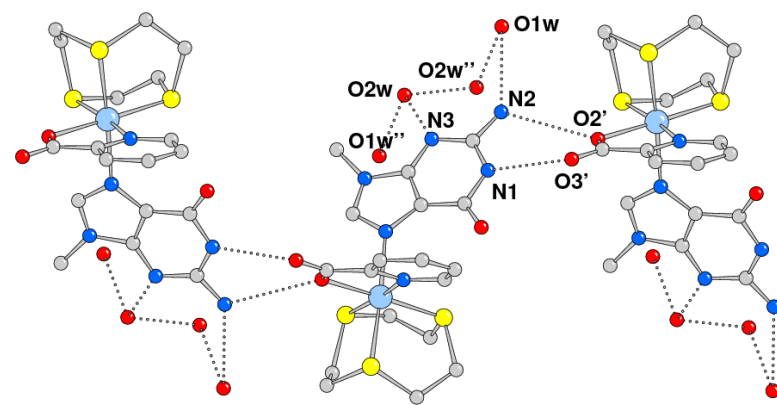


Figure S16. Crystal packing of complex $[\text{Ru}([\text{9}] \text{aneS3})(\text{pic})(\text{9MeG-}N7)](\text{PF}_6)$ (**10**) showing the chain built by intermolecular H-bonds along the *a*-axis (atoms ('') at $x, -y+1/2, z+1/2$; ('') at $1-x, 1-y, 1-z$).

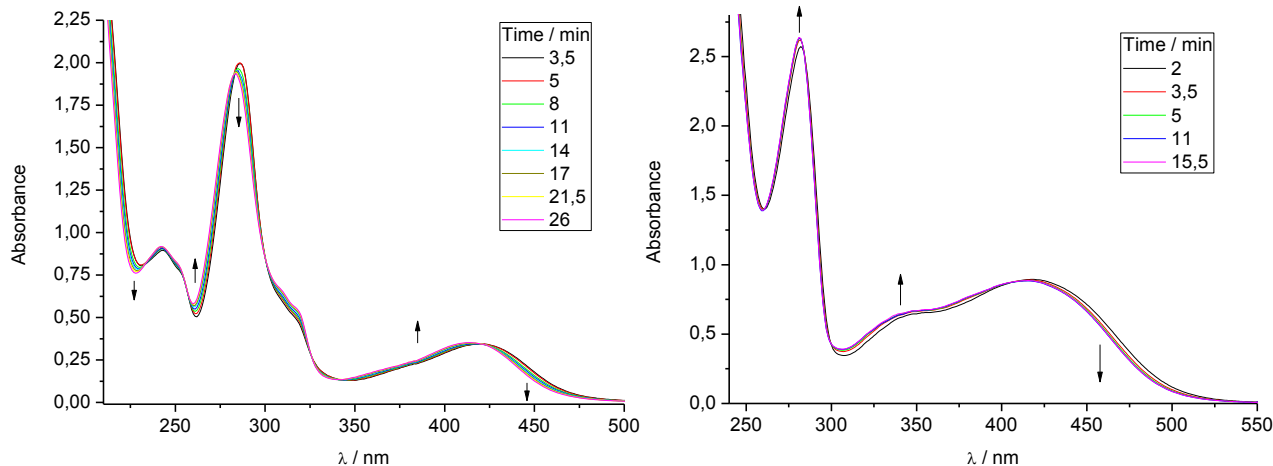


Figure S17. Time evolution of UV-Vis spectra during the aquation of the complex $[\text{Ru}(\text{[9]aneS}_3)(\text{bpy})\text{Cl}](\text{PF}_6)$ (**2**, left) and $[\text{Ru}(\text{[9]aneS}_3)(\text{pic})\text{Cl}]$ (**3**, right) in 0.1 M NaClO_4 at 298 K.

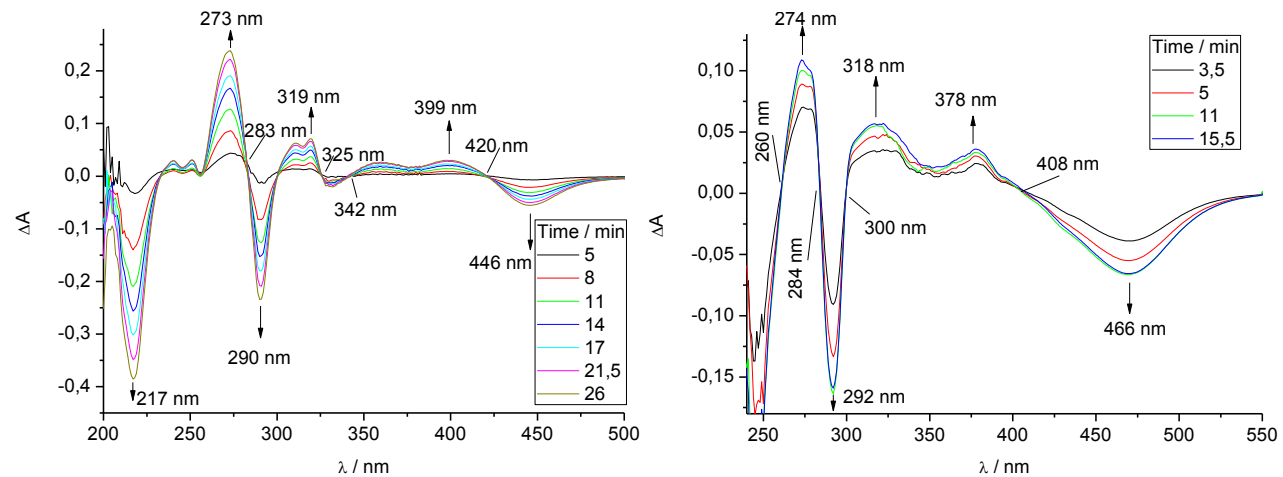


Figure S18. Time evolution of UV-Vis difference spectra during the aquation of the complex $[\text{Ru}(\text{[9]aneS}_3)(\text{bpy})\text{Cl}](\text{PF}_6)$ (**2**, left) and $[\text{Ru}(\text{[9]aneS}_3)(\text{pic})\text{Cl}]$ (**3**, right) in 0.1 M NaClO_4 at 298 K. $\Delta A = A_t - A_0$, where A_t = absorbance at time t and A_0 = absorbance at the time at which the first spectrum was recorded.

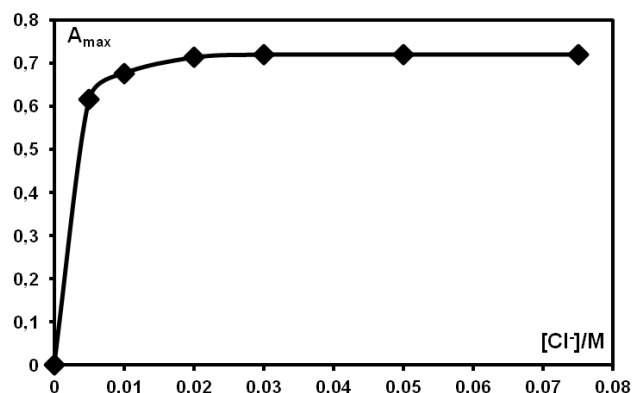


Figure S19. The change of absorbance at 446 nm of the complex $[\text{Ru}([\text{9}] \text{aneS}_3)(\text{bpy})\text{Cl}](\text{PF}_6)$ (**2**) *vs.* $[\text{Cl}^-]$ in 0.1M NaClO_4 at 310 K.

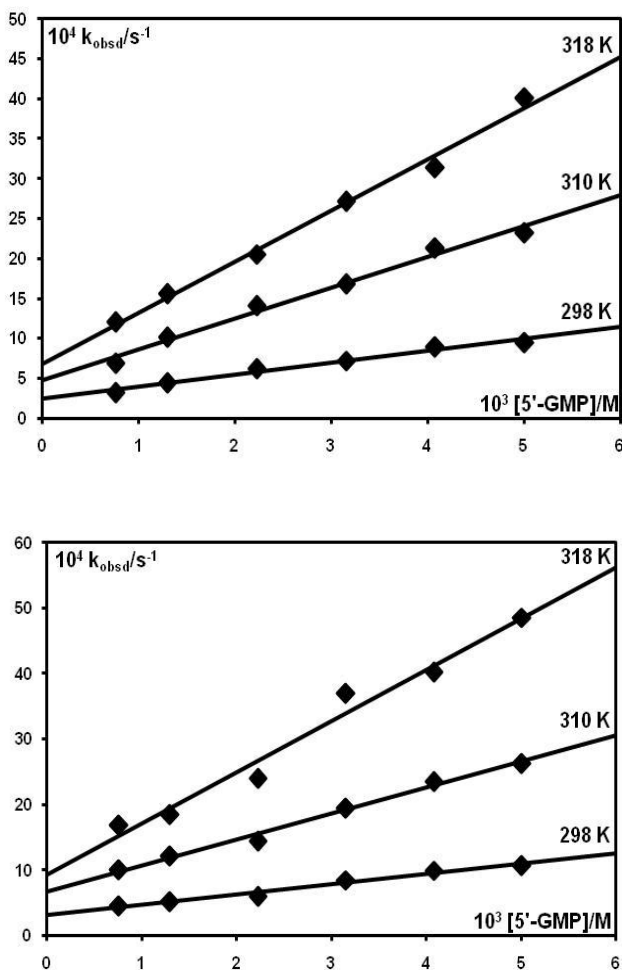


Figure S20. *Pseudo* first-order rate constants, k_{obs} , as a function of ligand concentration and temperature for the substitution reactions of $[\text{Ru}(\text{[9]aneS}_3)(\text{bpy})\text{Cl}](\text{PF}_6)$ (**2**, top), $[\text{Ru}(\text{[9]aneS}_3)(\text{pic})\text{Cl}]$ (**3**, bottom) with 5'-GMP in 25 mM Hepes buffer (30 mM NaCl, pH 7.2).

Table S1. Selected chemical shifts for the guanine derivatives 9MeG, Guo and 5'-GMP and for the products from their reactions with **1 – 3**.

species	pH	δ (H8)	δ (H1')	δ (CH ₃)	δ (H6)	δ (H5)	δ (H4)	δ (H3)	δ (³¹ P)
2					9.05 ^a	7.63 ^b	8.13 ^c	8.47 ^d	
2a					9.12 ^a	7.68 ^b	8.19 ^c	8.51 ^d	
3					8.94	7.68	8.09-8.07	8.09-8.07	
3a					9.02	7.73-7.69	8.13	8.13	
9MeG	7.60/ 7.88/ 7.73	7.74		3.65					
4	7.60	8.22		3.67					
7	7.88	7.98		3.47	9.29 ^a	7.69 ^b	8.13 ^c	8.36 ^d	
10	7.73	8.01		3.63	9.21	7.63	8.00	7.92	
Guo	7.63/ 7.74/ 7.70	7.99	5.90						
5	7.63	8.51	5.94						
8	7.74	8.25	5.77		9.26/9.24 ^a	7.69 ^b	8.13 ^c	8.35 ^d	
11	7.70	8.30/8.28	5.90/5.89		9.20	7.71	8.00	7.92	
5'-GMP	7.60	8.20	5.92						3.63
	3.30	8.38	5.97						0.16
	7.65	8.19	5.92						3.58
	7.95	8.21	5.93						3.71
6a	7.60	8.15	5.91						9.29
6b	7.60	8.66	5.95						3.85
	3.30	8.56	5.98						0.20
9	7.65	8.07	5.69		9.34/9.32 ^a	7.78/7.71 ^b	8.11 ^c	8.29 ^d	3.81
12	7.95	8.21/8.18	5.84/5.82		9.22	7.64	7.98	7.90	3.80/3.79

^a δ (H6/6'); ^b δ (H5/5'); ^c δ (H4/4'); ^d δ (H3/3')

Table S2. Species distribution for complexes **2** and **3** in 0.1 M NaClO₄ solution at equilibrium at 298 K under biologically relevant Cl⁻ concentrations.^[a]

Complex	[Cl ⁻] [mM]		% species	
			parent	aqua
[Ru([9]aneS ₃)(en)Cl] ⁺ (1) ^[b]	104	plasma	79.3	20.7
	22.7	cytoplasm	45.5	54.5
	4	nucleus	13.0	87.0
[Ru([9]aneS ₃)(bpy)Cl] ⁺ (2)	104	plasma	83.5	16.5
	22.7	cytoplasm	52.6	47.4
	4	nucleus	16.6	83.4
[Ru([9]aneS ₃)(pic)Cl] (3)	104	plasma	57.8	42.2
	22.7	cytoplasm	23.0	77.0
	4	nucleus	5.1	94.9

^[a] Initial concentration of the chlorido complexes is 80.0 μM, i.e. the IC₅₀ value calculated for the more active complex **1**.³

^[b] Results based on the *K* value of **1** obtained from the NMR experiments, i.e. *K*_{aq} = 27.2 × 10⁻³ M.

³ I. Bratsos, E. Mitri, F. Ravalico, E. Zangrandi, T. Gianferrara, A. Bergamo and E. Alessio, *Dalton Trans.*, 2012, **41**, 7358-7371.

Table S3. Observed *pseudo*-first order rate constants as a function of ligand concentration and temperature for the substitution reactions between complex [Ru([9]aneS₃)(en)Cl](PF)₆ (**1**) and 5'-GMP in 25 mM Hepes buffer (30 mM NaCl, pH 7.2).

λ [nm]	T [K]	[5'-GMP] [10 ⁻³ M]	k_{obs} [10 ⁻⁴ s ⁻¹] ^[a]
299	298	5.00	3.49 (2)
		4.08	2.83 (3)
		3.15	2.23 (2)
		2.22	1.58 (2)
		1.30	0.90 (2)
		0.74	0.72 (3)
310	310	5.00	9.05 (2)
		4.08	7.77 (2)
		3.15	5.10 (3)
		2.22	3.73 (3)
		1.30	2.59 (3)
		0.74	1.90 (3)
318	318	5.00	16.83 (3)
		4.08	14.46 (2)
		3.15	10.39 (2)
		2.22	7.79 (2)
		1.30	5.06 (3)
		0.74	2.96 (3)

^[a] Number of runs in parenthesis

Table S4. Observed *pseudo*-first order rate constants as a function of ligand concentration and temperature for the substitution reactions between complex $[\text{Ru}([\text{9}]\text{aneS}_3)(\text{bipy})\text{Cl}](\text{PF}_6)$ (**2**) and 5'-GMP in 25 mM Hepes buffer (30 mM NaCl, pH 7.2).

λ [nm]	T [K]	[5'-GMP] [10^{-3} M]	k_{obs} [10^{-4} s $^{-1}$] ^[a]
297	298	5.00	9.42 (2)
		4.08	8.88 (3)
		3.15	7.21 (2)
		2.22	6.17 (2)
		1.30	4.45 (2)
		0.74	3.15 (3)
310	310	5.00	23.17 (2)
		4.08	21.30 (2)
		3.15	16.75 (3)
		2.22	14.10 (3)
		1.30	10.09 (3)
		0.74	6.90 (3)
318	318	5.00	40.08 (3)
		4.08	31.37 (2)
		3.15	27.11 (2)
		2.22	20.52 (2)
		1.30	15.52 (3)
		0.74	12.01 (3)

^[a] Number of runs in parenthesis

Table S5. Observed *pseudo*-first order rate constants as a function of ligand concentration and temperature for the substitution reactions between complex [Ru([9]aneS₃)(pic)Cl] (**3**) and 5'-GMP in 25 mM Hepes buffer (30 mM NaCl, pH 7.2).

λ [nm]	T [K]	[5'-GMP] [10 ⁻³ M]	k_{obs} [10 ⁻⁴ s ⁻¹] ^[a]
295	298	5.00	10.71 (2)
		4.08	9.96 (3)
		3.15	8.48 (2)
		2.22	5.94 (2)
		1.30	5.15 (2)
		0.74	4.51 (3)
310	310	5.00	26.27 (2)
		4.08	23.54 (2)
		3.15	19.45 (3)
		2.22	14.46 (3)
		1.30	12.10 (3)
		0.74	9.99 (3)
318	318	5.00	48.56 (3)
		4.08	40.21 (2)
		3.15	36.91 (2)
		2.22	24.01 (2)
		1.30	18.52 (3)
		0.74	16.85 (3)

^[a] Number of runs in parenthesis